

Nonintrinsic origin of the magnetic-field-induced metal-insulator and electronic phase transitions in graphite

José Barzola-Quiquia,^{1,*} Pablo D. Esquinazi,^{1,†} Christian E. Precker,¹ Markus Stiller,¹ Mahsa Zoraghi,^{1,‡} Tobias Förster,² Thomas Herrmannsdörfer,² and William A. Coniglio³

¹*Division of Superconductivity and Magnetism, Felix-Bloch-Institut für Festkörperphysik, Universität Leipzig, Linnéstrasse 5, D-04103 Leipzig, Germany*

²*Hochfeld-Magnetlabor Dresden (HLD-EMFL), Helmholtz-Zentrum Dresden-Rossendorf, D-01328 Dresden, Germany*

³*National High Magnetic Field Laboratory, 1800 E. Paul Dirac Dr., Tallahassee, Florida 32310-3706, USA*

(Dated: February 4, 2019)

A detailed magnetoresistance study of bulk and microflake samples of highly oriented pyrolytic graphite with a thickness of 25 μm to 23 nm reveals that the usually observed field-induced metal-insulator and electronic phase transitions vanish in thinner samples. The observed suppression is accompanied by orders of magnitude decrease of the magnetoresistance and of the amplitude of the Shubnikov-de-Haas oscillations. The overall behavior is related to the decrease in the quantity of two-dimensional interfaces between crystalline regions of the same and different stacking orders present in graphite samples. Our results indicate that these field-induced transitions are not intrinsic to the ideal graphite structure and, therefore, a relevant portion of the published interpretations should be reconsidered.

In the early 1980's, Tanuma et al. reported a sharp increase in the magnetoresistance (MR) of graphite when a strong magnetic field $\mu_0 H \geq 20$ T is applied parallel to the c -axis at temperatures $T < 10$ K [1]. Later, this observation was confirmed in different kinds of graphite samples, e.g. in Kish graphite [2–8], synthesized as a byproduct in steelmaking, and in highly oriented pyrolytic graphite (HOPG) [9–11]; for recent reviews see [12, 13]. There are a number of theoretical studies trying to provide an answer to several details of the electronic transitions observed in graphite at high fields and low temperatures. Yoshioka and Fukuyama [14], for example, proposed the existence of charge-density waves or spin-density waves to explain such electronic anomalies. Also, an excitonic BCS-like state was proposed to understand the behavior observed at fields above 50 T [3]. Recently, the field-induced metal-insulator transition in thin flakes of Kish graphite with thickness $t = 178$ nm and 70 nm were studied [7], also under the influence of an electric field [8]. Those results were tentatively interpreted suggesting that the electronic state in the insulating phase has an order along the stacking c -axis direction [8].

Several unclear experimental details of the field dependence of the electrical resistance of graphite samples added to the different interpretations demonstrate that there is no consent on the origin of the field-induced transitions. Part of the reason is related not only on details of the proposed phase diagram [12, 13] but to conflicting experimental evidence, as for example that the electronic transitions are sometimes absent in certain ordered graphite samples [9, 15]. In this letter we show that these

high-field transitions as well as the metal-insulator transition are not intrinsic of the graphite ideal structure but related to internal two-dimensional (2D) interfaces.

We start by pointing out a misleading assumption used in the related literature, namely, that the measured electrical properties of graphite correspond to the one of a homogeneous (structurally and electrically) graphite sample [16]. Graphite is a layered material built by weakly coupled graphene sheets, where usually the graphene layers adopt a hexagonal $ABABA\dots$ (2H) stacking sequence (Bernal) [17] or as a minority phase the $ABCABCA\dots$ stacking order (rhombohedral (3R)) [18]. Scanning transmission electron microscopy (STEM) measurements show that most of the samples are formed by a stacking of crystalline blocks with well defined interfaces between them, see the upper right inset in Fig. 1, as example. In general, three types of interfaces can be found, namely, between twisted 2H crystalline regions (we name it type I); between twisted 3R regions (type II) and between (twisted) 3R/2H regions (type III). The twist angle θ_t between the two crystalline regions of an interface is defined through a rotation around the common c -axis (see, e.g., [19]). It may play a main role in the electronic properties of a given interface. For example, Van Hove singularities in the density of states are situated closer to the zero bias energy at smaller θ_t [20], or a flat band is expected at $\theta_t = 0^\circ$ for a type III interface [21, 22]. The thickness of the crystalline regions (in the c -axis direction) having a common interface varies between ~ 10 nm to ~ 500 nm upon sample and location within the same sample. Electron back scattering diffraction (EBSD) indicates that the lateral sizes of those crystalline regions in HOPG samples range between ~ 1 μm to ~ 20 μm [23].

Earlier experimental studies reported the vanishing of the Shubnikov-de-Haas (SdH) oscillations amplitude the thinner the Kish graphite sample [24, 25]. Furthermore, a nonlinear increase of the resistance of graphite samples by decreasing their thickness was reported [26], i.e.,

* j.barzola@physik.uni-leipzig.de

† esquin@physik.uni-leipzig.de

‡ Current address: Department of Neurophysics, Max Planck Institute for Human Cognitive and Brain Sciences, 04103 Leipzig, Germany

the absolute resistivity increases the thinner the sample [27, 28]. All this experimental evidence is at odd with the hypothesis of homogeneity assumed in most of the investigations of the electronic transport properties of graphite and speaks for an unconventional contribution of interfaces embedded within a semiconducting matrix. We further note that superconductivity at ~ 1 K was discovered in a single interface, a twisted bilayer graphene [29]. Additionally, evidence for granular superconductivity with much higher critical temperatures at embedded interfaces in bulk HOPG and natural graphite samples was reported earlier [30–33]. Therefore, we expect that the main MR signal measured at low enough temperatures and thick enough graphite samples should be mainly related to the electronic systems within the 2D interfaces.

We studied the in-plane MR under pulsed magnetic fields $\mu_0 H \leq 62$ T (applied parallel to the c -axis) in four different samples with thickness between $23 \text{ nm} \leq t \leq 25 \text{ }\mu\text{m}$ and lateral size from mm to below $10 \text{ }\mu\text{m}$, obtained from a millimeter size HOPG sample from Advanced Ceramics (grade A). Further sample details and measuring techniques are given in the supplementary information (SI). The MR measurements under pulsed fields were accompanied by the temperature dependence of the resistance $R(T)$ and MR measurements under stationary magnetic fields to 18 T, shown in the SI.

Figure 1 shows the temperature dependence of the resistance $R(T)$ of all four samples without applied field. In the inset of Fig. 1 the resistivity ρ is plotted as a function of sample thickness t . The temperature dependence of the electrical resistance can be very well understood assuming the parallel contribution of semiconducting regions with both stable stacking orders and a metalliclike contribution from the interfaces [28, 34, 35], as shown by the fits to the data in Fig. 1. Whereas the resistance of the thickest sample shows the typical metalliclike behavior of bulk graphite, the $R(T)$ of the microflakes tends to a semiconductinglike behavior the smaller the sample thickness. The change from metalliclike to semiconductinglike behavior, decreasing sample thickness, is due to the reduction of the number of highly conducting 2D interfaces [28]. Obviously, the (low) field-induced metal-insulator transition does not occur in thin graphite samples. The $R(T)$ curves shown in Fig. 1, as well as those obtained in more than 20 samples from different origins and measured in different laboratories, can be very well described between 2 K and 1100 K with a parallel resistor model [28, 34, 35]. The difference in the fit parameters of the four samples shown in Fig. 1 is mainly in the total conductance of the interfaces, decreasing the thinner the sample [28, 35].

We now discuss the magnetoresistance, defined as $\text{MR} = (R(H) - R(0))/R(0)$, at different temperatures shown in Fig. 2 for the bulk sample. In general, at $T \gtrsim 150$ K the contribution of the interfaces to the total MR starts to be overwhelmed by the higher conductance of the two semiconducting phases contributing in paral-

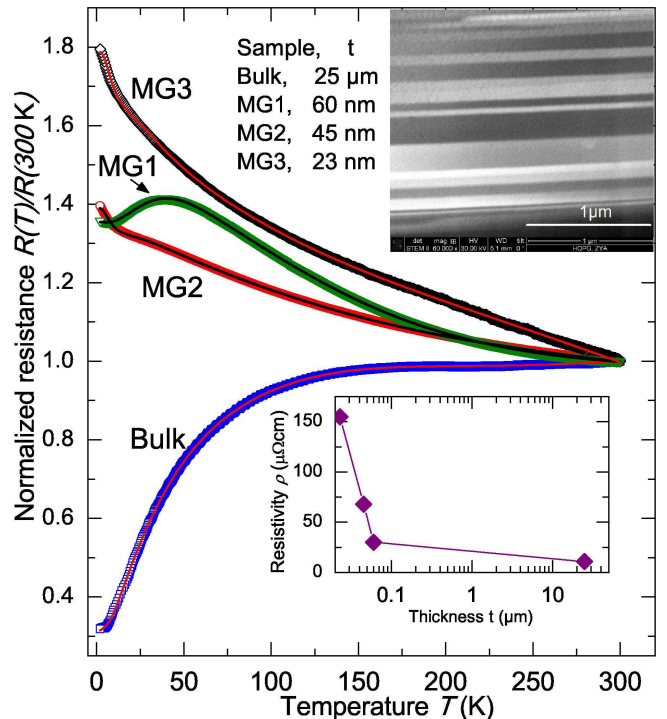


Fig. 1. Normalized resistance of the investigated samples vs. temperature. The lines through the data points are fits to the three contributions in parallel as described in detail in Refs. [28, 34, 35]. The main change between the bulk and the thinner flakes is given by the weight of the metalliclike interfaces conductance. The inset at the bottom shows the resistivity as function of the thickness t at room temperature. The upper inset shows a STEM image with the e -beam parallel to the graphene planes of graphite. The c -axis of the graphite structure is normal to the interfaces existing between crystalline regions, shown with different brightnesses. Those regions correspond either to crystalline Bernal regions twisted around the common c -axis or to the rhombohedral phase. For further STEM pictures see [19].

el [35]. Therefore, at high enough temperatures the MR behaves as the one of a (low-gap) semiconductor. For graphite samples with lateral dimensions larger than the mean free path [36–38], the two-band model given by Eq. (1) and derived under the Boltzmann-Drude quasi-classical diffusive approach [39], provides a good (qualitative) description of the MR of bulk graphite at $T > 120$ K (dashed lines in Fig. 2). The equation

$$\text{MR} = \left[\mu^2 B^2 \left(1 - \frac{\Delta n^2}{n^2} \right) \right] / \left[1 + \mu^2 B^2 \frac{\Delta n^2}{n^2} \right], \quad (1)$$

is a simplified version of the two-band model equation assuming equal mobility for both electrons and holes ($\mu = \mu_e \approx \mu_h$), with $\Delta n/n = (n_e - n_h)/(n_e + n_h)$ the relative charge imbalance between electron n_e and hole n_h carrier densities and $B = \mu_0 H$. This simplified expression has only two adjustable fitting parameters, the average mobility μ and the relative charge imbalance $\Delta n/n$

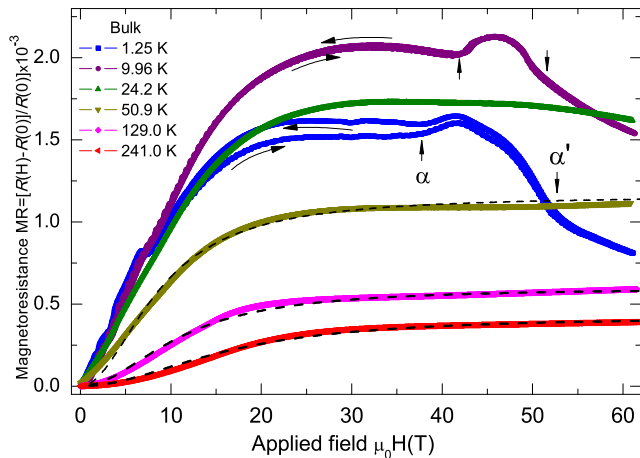


Fig. 2. High magnetic field results of the HOPG bulk sample ($t = 25 \mu\text{m}$). The vertical arrows indicate the “critical fields” $\alpha(T)$ and $\alpha'(T)$. The horizontal arrows indicate the field sweep direction. The dashed lines through the data points at the three highest temperatures are fits to Eq. (1) with the parameters $\Delta n/n = 0.0484$, and $\mu = 1.277 \text{ m}^2/\text{Vs}$ at $T = 241 \text{ K}$. At lower T , μ slightly increases whereas $\Delta n/n$ decreases, see SI for a discussion of the parameters. The best possible fit of the data at 50.9 K to Eq. (1) is shown only to emphasize the disagreement at low fields and the develop of a maximum at $\sim 30 \text{ T}$. The fits to Eq. (1) get much worse at lower T .

and it is insensitive to the absolute value of n_e (or n_h). Equation (1) provides two key features of the experimental MR, namely the B^2 field dependence at low fields and its saturation at high enough fields, see Fig. 2.

The MR data at $T \leq 50.9 \text{ K}$ shown in Fig. 2 deviate from the predictions of the two-band model (independently of the fitting parameters used in Eq. (1)): there is a linear field dependence at low fields and a maximum around 30 T develops. The negative MR at high fields becomes more pronounced the lower the temperature and, in addition, a clear bump between $\sim 35 \text{ T}$ and $\sim 55 \text{ T}$ appears. This behavior has been reported for Kish and HOPG graphite and it was attributed to field-induced phase transitions at T -dependent critical fields $\alpha(T)$ and $\alpha'(T)$ (indicated by vertical arrows in Fig. 2) [4, 6, 9, 12, 13]. We further note that the overall MR decreases at $T < 10 \text{ K}$. Also the absolute value of the resistance at high enough fields steadily decreases, i.e., $R(1.25 \text{ K}, 60 \text{ T}) \simeq 6 \Omega < R(241 \text{ K}, 60\text{T}) \simeq 9 \Omega$ (see Fig.S8 in the SI). This is attributed to the so-called reentrance to a metallic state in the quantum limit, originally shown and discussed in [40].

At low temperatures, a hysteresis in the MR emerges at $\approx 12 \text{ T}$ and vanishes at $\approx 50 \text{ T}$, being the MR smaller at the increasing field branch, see Fig. 2. The opening of a hysteresis at high fields was first mentioned by Takashi et al. [1] and further discussed in [41] using data from a Tanzanian natural graphite sample. We stress that such hysteresis in the MR is observed only at low temperatures

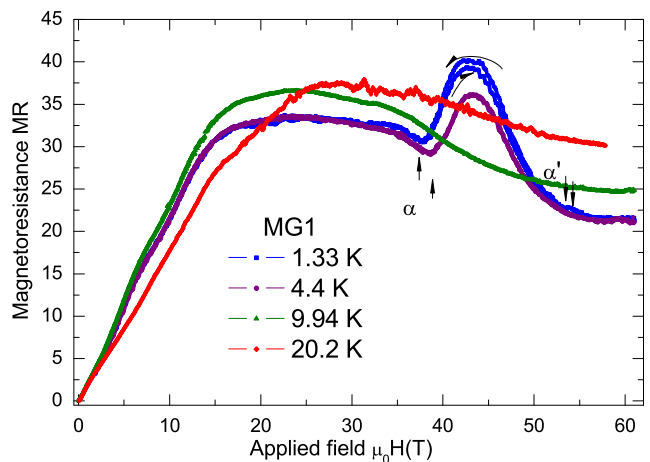


Fig. 3. High magnetic field magnetoresistance MR of sample MG1 ($t = 60 \text{ nm}$) at different temperatures. The vertical arrows indicate the critical fields $\alpha(T)$ and $\alpha'(T)$ and the horizontal arrows refer to the field sweep direction to emphasize the hysteresis observed only at the lowest temperature. At all other temperatures the curves are reversible in field within experimental resolution.

and only in thick enough samples (see also Fig. 3). See the SI for more details on the mentioned hysteresis.

We discuss the results of the thinner flakes. The MR results of sample MG1 ($t = 60 \text{ nm}$) are plotted in Fig. 3. One can clearly recognize the transitions at $\alpha(T)$ and $\alpha'(T)$. In general, the MR of this sample changes only slightly in the measured temperature range and behaves qualitatively similar to the bulk sample, in spite of two to three orders of magnitude smaller sample width and length (see SI). We note that the MR is ~ 2 orders of magnitude smaller than in the bulk sample. In addition to the (small) reduction of the MR due to the decrease of the lateral size (compared to the bulk sample [36]) the largest decrease of the MR is due to the decrease in the thickness and consequently in the amount of interfaces [28]. As in the bulk sample, a clear negative MR starts to appear at fields above $\sim 30 \text{ T}$ and the field dependence is linear at low fields.

Results of sample MG2 are plotted in Fig. 4. In contrast to the previous samples, no evident field transition $\alpha(T)$ is observed. At the lowest temperature we can recognize a α' transition only. In the field range between 30 T and 62 T and increasing T we observe a change from a negative to a positive MR. Note that the MR increases with T , without any sign of saturation at high fields, in clear contrast to the bulk sample. The MR is reversible within experimental resolution.

The results of the thinnest sample MG3 are shown in Fig. 5. Its MR is overall much smaller than in the other samples and, as in sample MG2, its MR increases with temperature with no sign of saturation. As in the other samples, at low enough T and fields above 30 T, a negative MR is observed to 50 T. The MR of this sample

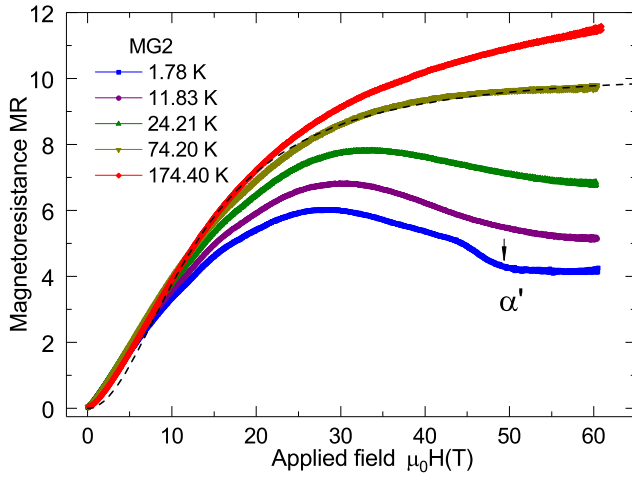


Fig. 4. High magnetic field magnetoresistance MR of sample MG2 ($t = 45$ nm) at different temperatures. The vertical arrow indicates the critical field $\alpha'(T = 1.78$ K). The dashed line is calculated from Eq. (1) to fit the high field MR data at 74.20 K, as example, although this equation is not really applicable due to non-diffusive, ballistic contribution, see text. Further, note the deviation of the data from the expected H^2 dependence at fields below 5 T.

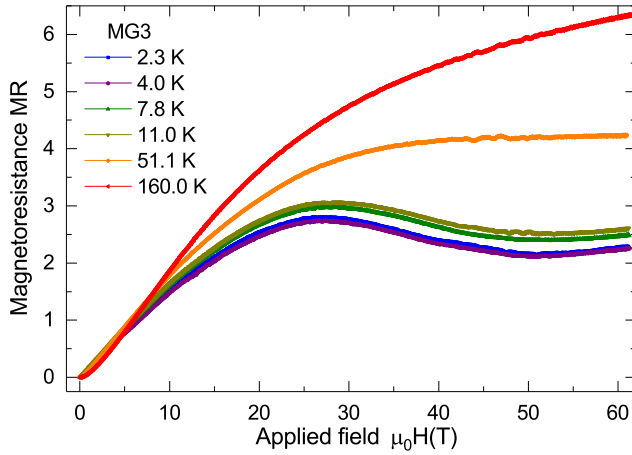


Fig. 5. High magnetic field MR of sample MG3 ($t = 23$ nm \sim 80 graphene layers) at different temperatures.

shows only a smooth feature between 40 T and 50 T, i.e., where the high field-induced transitions were observed in the other samples, and at the lowest temperature.

In what follows we provide an interpretation of the main results. We note that due to the different, partially unknown, parallel contributions to the MR (one from the interfaces, which includes different types, and two from the semiconducting layers [28, 34, 35]), the qualitative description we provide below uses the fact that the interfacial contribution to the total conductance overwhelms the other two at $T < 100$ K [35]. However, its influence on the MR weakens with fewer interfaces, as expected.

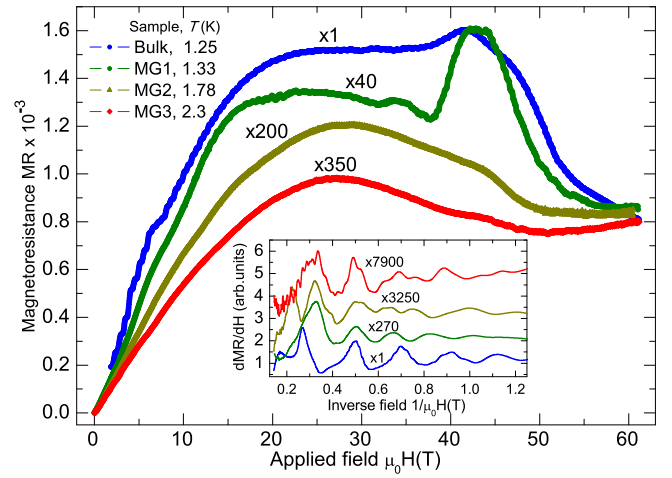


Fig. 6. Magnetoresistance of all samples investigated in this work at the lowest temperature. The inset shows the SdH oscillations obtained at $T = 5$ K. The numbers beside the curves are the multiplication factor to show the results in the same scale.

(1) The fact that the field-induced transitions at the fields $\alpha(T), \alpha'(T)$ systematically vanish the smaller the thickness of the samples (for similar lateral sample dimensions) indicates that these are not intrinsic of the ideal graphite structure. Taking into account previous galvanomagnetic studies [19, 27, 28, 34, 35], their suppression is related to the smaller quantity of certain internal interfaces. Our results and interpretation provide an answer to the absence of high-field electronic phase transitions in certain graphite samples mentioned in Refs. 9 and 15 as well as the scattering of the “critical fields” data.

(2) The vanishing of the field-induced transitions is accompanied by a large decrease in the absolute MR in the whole field range, see Fig. 6. The decrease in the MR by a factor ~ 700 between the bulk and MG3 is mainly related to the decrease in the amount of interfaces.

(3) The low-temperature MR curves in Fig. 6 suggest that the field-induced transitions are superposed with a MR curve that resembles that of the thinnest MG3 sample, i.e., the MR increases linearly in field at low fields, it reaches a maximum at $20 \text{ T} < \mu_0 H < 30 \text{ T}$ and shows a negative MR at $30 \text{ T} < \mu_0 H < 50 \text{ T}$ (see also Fig.S9 in the SI). This fact added to the clear deviation from the expected two-band model behavior given by Eq. (1) suggest that even the behavior of the thinnest sample MG3 at low temperatures is not yet intrinsic of the graphite ideal structure. Note that the SdH oscillations measured in graphite samples are not intrinsic but related to certain interfaces [28]; these are observed in all samples, see inset in Fig. 6. However, the decrease of the amplitude of the SdH oscillations (characterized by the first field derivative of the MR) is more than 10 times larger than the decrease in the MR itself, suggesting that the MR of the graphite samples

results from contributions of different interfaces or different regions within same interfaces. A considerable amount of extensive experimental work needs to be done to characterize the contribution(s) of each kind of interfaces to the total MR.

(4) Taking into account that certain interfaces can have granular superconducting properties in a broad temperature range [19, 29–33], the linear MR at low fields as well as the negative MR at $30 \text{ T} < \mu_0 H < 50 \text{ T}$ may be related to the influence of the applied field to the Josephson coupled superconducting regions. We note that the normalized resistance data of our samples resemble the behavior observed as a function of field in granular low- T_c superconductors, as AlGe [42] or InO [43], see discussion in Sec. II.A and Fig.S9 in the SI. We refer the reader to the related literature [44, 45].

(5) Earlier experiments in thin graphite samples with no or a low number of interfaces showed that the mean free path of the carriers within the graphene layers can be several microns large [37], of the order of our samples lateral size. In this case a ballistic, not the diffusive regime assumed in Eq. (1), should be taken into account to understand the non saturation of the MR at high fields observed in the MG2 and MG3 samples (Figs. 4 and 5). The increase of the MR with temperature at all fields, as in the thinner samples MG2 and MG3, is observed because the carriers mean free path, of the order of sample lateral size, decreases with temperature [36, 37].

(6) Finally, we note that the MR oscillations periodic in field and the behavior under a bias voltage recently reported in thin graphite samples [8] were already observed earlier and their origins are related to the existence of 2D interfaces and granular superconductivity [46, 47].

Magnetoresistance measurements of graphite samples of different thickness in a wide temperature and field range indicate that the reported field-induced electronic phase transitions are not intrinsic of the ideal graphite structure but related to 2D electronic systems localized at certain interfaces formed between the crystalline regions, commonly found in graphite samples with thickness above a few tens of nanometers. Our conclusion is also supported by the thickness dependence observed in other galvanomagnetic characterizations. We encourage the scientific community to revise the theoretical interpretations of the high-field transitions published in the past and to take into account explicitly the different kinds of possible interfaces graphite samples have.

Acknowledgements: We gratefully acknowledge A. Gerber (Tel Aviv University) and A. A. Varlamov (Istituto Superconduttori, Rome) for useful discussions on granular superconductivity and fluctuation effects, and P.K. Muduli for discussion on the two-band model. C.E.P. gratefully acknowledges the support provided by the Brazilian National Council for the Improvement of Higher Education (CAPES) under 99999.013188/2013-05. The studies were supported by the DAAD Nr.

57207627 (“Untersuchungen von Grenzflächen in Graphit bei sehr hohen Feldern”) and partially supported by the DFG under ES 86/29-1 and the SFB 762. A portion of this work was performed at the National High Magnetic Field Laboratory, which is supported by National Science Foundation Cooperative Agreement No. DMR- 1157490 and the State of Florida. We acknowledge the support of the HLD at HZDR, member of the European Magnetic Field Laboratory (EMFL).

Supplementary information to: “Nonintrinsic origin of the magnetic-field-induced metal-insulator and electronic transitions in graphite”

I. SUMMARY OF SAMPLES DIMENSIONS AND PREPARATION DETAILS OF THE SAMPLES SHOWN IN THE MAIN MANUSCRIPT

The graphite microflakes were produced by a rubbing method described in a previous publication [27]. After patterning the electrodes geometry for the resistance measurements using electron beam lithography, the voltage and input current electrodes on the samples were produced by sputtering of Cr/Au. Table I shows the dimensions of the four samples shown in the main manuscript. All samples were from the same bulk HOPG sample of grade A. All measurements were done in a four-probe configuration and magnetic fields were applied along the c -axis direction of the graphite structure. The temperature dependence of the resistance and the low field MR were initially characterized using a commercial ^4He cryostat. The high magnetic fields magnetoresistance (MR) was measured at the high magnetic field laboratory in Dresden (to 62 T applied with a pulse length of ~ 150 ms) and in Tallahassee (DC fields to 18 T) within the temperature range of 1.2 K to 245 K. A Lock-in amplifier (3.33 kHz) was used to measure the voltage during the rise and decay of the magnetic field. The applied currents varied between 5 μA to 10 μA to avoid self heating effects.

In general, HOPG samples of grade A thicker than $\gtrsim 100$ nm show transport properties similar to bulk graphite. With exception of [7, 8], most of the previous studies on the high field MR of graphite were done on thicker samples of millimeter size [1–5, 9, 11, 14]. Taking into account the internal structure of the graphite samples [19, 23, 34] (see Fig.1 in the main manuscript), we need to reduce the sample thickness to tens of nanometers and also the lateral size to a few micrometers in order to get electrical properties nearer to the intrinsic one of ideal, single phase graphite.

II. RESULTS UNDER DC APPLIED FIELDS

A. Temperature dependence of the magnetoresistance at fields $\leq |\pm 7|$ T

We first present the results at low fields in the range ± 7 T. The obtained results are plotted in Fig.S1 to Fig.S 4. In panels (a) we show the MR at different constant temperatures and in panels (b) the temperature dependence of the MR at the fixed field of 7 T. The temperature dependence of the resistance at zero field is shown in Fig.1 of the main article. As pointed out in the main article, the MR systematically decreases the smaller the

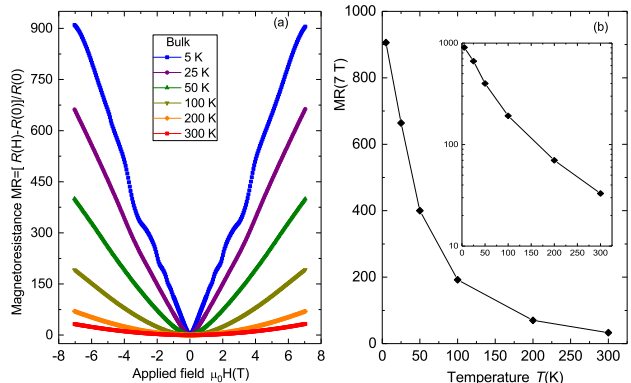


Fig.S1. (a) Magnetoresistance of the bulk sample bulk measured at different constant temperatures. (b) The temperature dependence of the MR at a fixed field of 7 T. Its inset shows the same data but in a semilogarithmic scale.

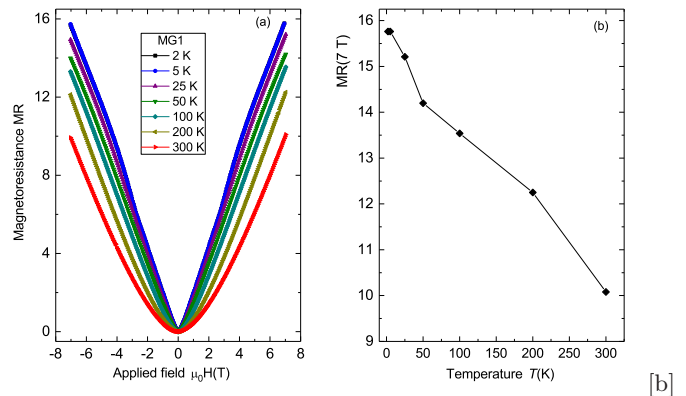


Fig.S2. (a) Magnetoresistance of the graphite flake MG1 measured at different constant temperatures. (b) The temperature dependence of the MR at a fixed field of 7 T.

sample thickness. The main reason for this decrease is not the change in the lateral size of the samples, which remains basically the same between samples MG1, MG2 and MG3, but the decrease in the quantity of 2D interfaces. Interesting is also the temperature dependence of the MR at constant field shown in panels (b). Whereas for the thicker sample the MR at 7 T decreases by a factor of 30 between 5 K and 300 K, see Fig. 1(b), this decrease with T strongly diminishes for sample MG1 to a factor 1.6, see Fig. 2(b), and gets non-monotonous and overall much smaller for samples MG2 and MG3, see Fig. 3(b) and Fig. 4(b). Note that there is a relatively larger decrease of the MR with T below 100 K for samples bulk and MG1, i.e., in the region where the 2D interfaces contribution overwhelms the contribution of the semiconducting paths. The non-monotonous tem-

Sample name	Length l (m)	Width w (m)	Thickness t (m)	$R(300\text{K})$ (Ω)
Bulk	0.0035	7×10^{-4}	2.5×10^{-5}	0.023
MG1	4×10^{-6}	7×10^{-6}	6×10^{-8}	2.926
MG2	4×10^{-6}	9×10^{-6}	4.5×10^{-8}	6.7
MG3	6×10^{-6}	8×10^{-6}	2.3×10^{-8}	50.7

TABLE I. Summary of samples dimensions and the absolute resistance at 300 K.

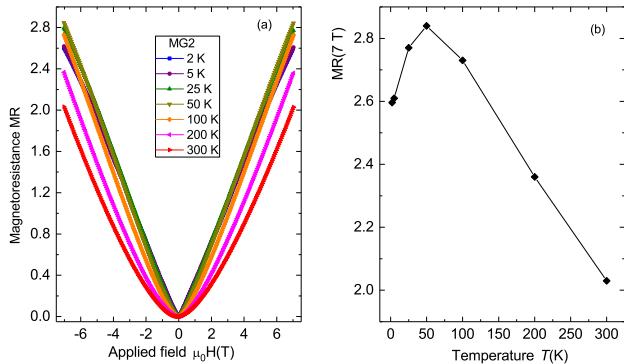


Fig.S3. a) Magnetoconductance of the graphite flake MG2 measured at different constant temperatures. (b) The temperature dependence of the MR at a fixed field of 7 T.

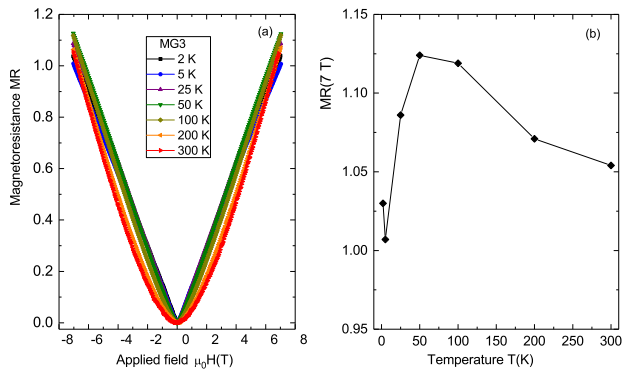


Fig.S4. a) Magnetoconductance of the graphite flake MG3 measured at different constant temperatures. (b) The temperature dependence of the MR at a fixed field of 7 T.

perature behavior of $MR(T)$ below 100 K in the thinner samples MG2 and MG3 is related to the temperature dependent decrease of the carriers mean free path $\ell(T)$ in the mainly semiconducting regions and the non-diffusive, ballistic transport that applies when $\ell(T)$ is of the order of the samples lateral size [37, 38]. The maximum in the $MR(T)$ shifts to higher temperatures the higher the applied magnetic field, see Figs. 4 and 5 in the main manuscript.

To understand all the observed effects we need to take into account: (a) the large carrier mean free path of the carriers at the semiconducting graphene layers, which is comparable to the sample size, (b) the large Fermi wave-

length λ_F due to the low carrier density, (c) the decrease with T of λ_F at the semiconducting regions, and (d) the cyclotron radius r_c , which reduces with magnetic field [36, 37]. As discussed in [36] the MR vanishes when $\lambda_F \gg r_c$. We stress that the conduction mechanism in graphite samples occurs along the graphene layers and interfaces, there is no surface scattering. The electron mean free path in thin graphite flakes is of the order of micrometers for samples with thickness smaller than ~ 50 nm [37, 38]. The transport in the c -axis direction, normal to the graphene planes, is negligible due to the very weak coupling between the graphene planes in graphite. In fact, the MR depends only on the field component normal the graphene and interfaces planes. Deviations from this normal field component are due to intrinsic and/or extrinsic misalignments of the single crystallites within the graphite samples.

Note that the linear in field MR is observed at low enough temperatures and in all samples. Whether this linear in field dependence of the MR is intrinsic of the graphite structure or related to granular superconductivity is not yet clear, see the discussion in Section V below. We stress that even in the thinnest sample the contribution of the interfaces is still measurable at low enough temperatures, as the overall field dependence of the MR (with a maximum at a certain high field) and the existence of the SdH oscillations indicate, see Fig.6 in the main manuscript and its inset. We would like to note that the linear in field magnetoconductance is a subject discussed in a large number of publications. The linear in field dependence of the longitudinal resistance is very often invoked as evidence for exotic quasiparticles in new materials. On the other hand linear magnetoconductance has been measured in “simple” semiconducting samples like Mn implanted Ge [48] or in 2D electron gas in an ultrahigh mobility GaAs quantum well [49]. Experimental evidence suggests that its origin can be an admixture of a component of the Hall resistivity to the longitudinal resistance related to density fluctuations, which exist in nearly every sample, especially when the carrier density is low [49].

B. The temperature dependence of the resistance and MR at fields $\leq |\pm 18|$ T

Table II shows the dimensions of two more samples measured to ± 18 T. The temperature dependence of the resistance $R(T)$ at different constant fields as well as the

Sample name	Length l (m)	Width w (m)	Thickness t (m)	$R(100\text{K})$ (Ω)
BSR (bulk)	0.0032	1.03×10^{-3}	5×10^{-5}	0.00515
MG-P1	14.5×10^{-6}	8.3×10^{-6}	10×10^{-8}	5.69

TABLE II. Summary of the dimensions of two more graphite samples, which MR was measured to ± 18 T. The BSR sample was a natural graphite and sample MG-P1 was prepared from a HOPG, grade A bulk sample.

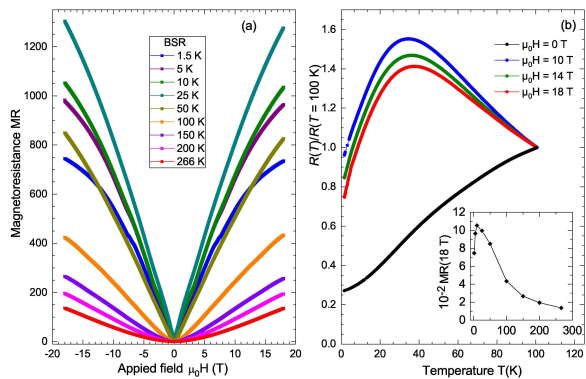


Fig.S5. (a) Magnetoresistance and in (b), the temperature dependence of the resistance $R(T)$ at different constant applied fields of a second bulk graphite sample, see Table II. The inset shows the $MR(18\text{ T})$ vs. temperature.

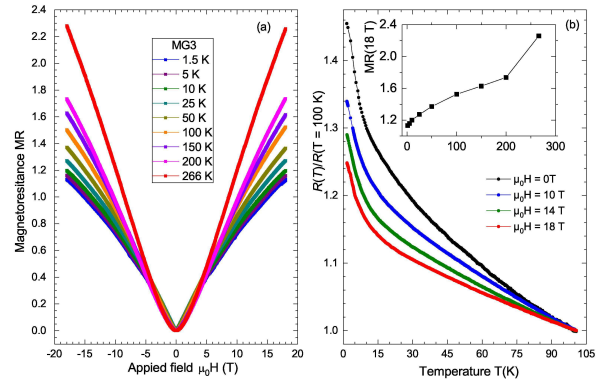


Fig.S7. (a) Magnetoresistance and in (b), the temperature dependence of the resistance $R(T)$ at different constant applied fields of the same flake MG3 measured with pulsed fields. Both sets of data are similar. The inset shows the $MR(18\text{ T})$ vs. temperature.

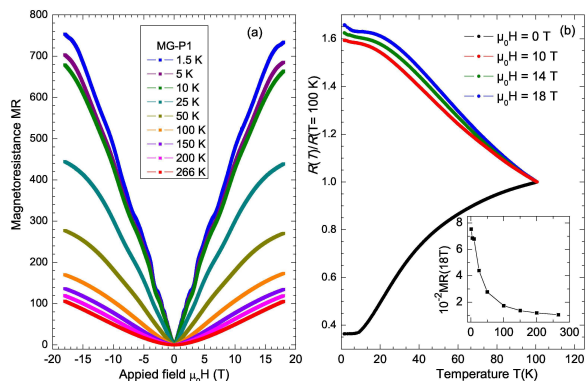


Fig.S6. (a) Magnetoresistance and in (b), the temperature dependence of the resistance $R(T)$ at different constant applied fields of the graphite flake (100 nm thick) MG-P1, see Table II. The inset shows the $MR(18\text{ T})$ vs. temperature.

magnetoresistance MR results are plotted in Fig.S5 to Fig.S7. Similar to the bulk HOPG sample shown in the main manuscript and above, the bulk BSR sample shows a huge MR, which diminishes increasing the temperature. In the inset of Fig.S5(b) we have plotted the $MR(18\text{ T})$ as a function of temperature. Its behavior is similar to other thick HOPG or Kish graphite samples. The $R(T)$ results

under applied fields of the bulk sample BSR shows the already reported reentrance to a metalliclike state at high enough fields and low enough temperatures, observed in HOPG bulk graphite samples[50]. We would like to remark that such reentrance behavior is also thickness dependent. It is clear to see the metalliclike behavior up to 30 K in the bulk sample (see Fig.S5 (b)) at the applied fields. While in the case of the thicker flake (see Fig.S 6(b)) a smooth but evident metalliclike behavior develops at $T < 20$ K. In the thinnest flake MG3 and at all investigated fields no reentrance behavior is observed (see Fig.S7(b)). All this evidence points out that the origin for the reentrance is related to the magnetic response of certain interfaces existent in thick enough samples.

III. THE REENTRANCE TO A METALLICLIKE STATE AT HIGH MAGNETIC FIELDS IN THICK GRAPHITE SAMPLES

The reentrance to a metalliclike state shown in Fig.S 5(b) has been shown originally in Ref. 50 and a possible explanation was given in terms of the enhancement of the density of states by the applied field and the possibility that superconducting correlations appear [50, 51]. Note that at the time of those publications the contribution of the embedded interfaces to the conductance of graphite samples was not known and therefore it was not consid-

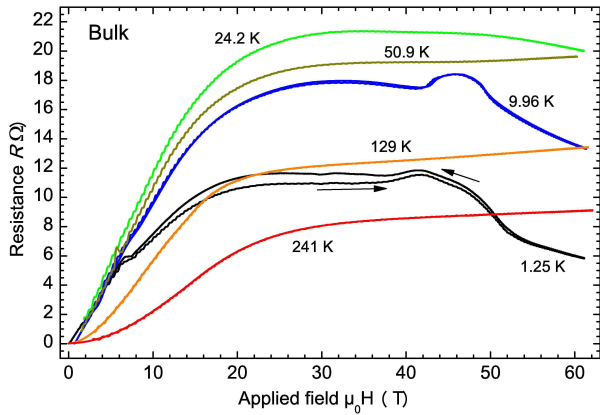


Fig.S8. Absolute resistance vs. magnetic field at different constant temperatures of the same bulk sample shown in the main manuscript.

ered in the proposed explanations. We would like to point out here that the observed reentrance provides a further evidence for the different contributions in parallel, i.e., for the inhomogeneous nature of thick graphite samples. To understand this point, the best is to plot the data of Fig. 2 of the main manuscript in absolute resistance values, instead of the MR, as shown in Fig.S8. In this figure we note that the absolute resistance at 1.25 K and at fields above 50 T gets *smaller* than the resistance at 241 K at the same fields. This fact is very difficult to understand were the sample homogeneous, independently of the reason for the negative resistance that develops above 30 T and at low enough temperatures. However, if we consider that at 241 K the measured resistance is basically due to the semiconducting regions and at 1.25 K those semiconducting regions are effectively short circuited by the interfaces, the observed behavior is much easier to be understood, assuming that the maximum and the negative MR is a phenomenon that exists only at certain high conducting interfaces. A short discussion on the negative MR observed at high enough fields and low enough temperatures is given in Section VI.

IV. PARAMETERS OF THE TWO-BAND MODEL AND THE FIELD DEPENDENCE OF THE MR

The field dependence of the resistance measured at high enough temperatures, as shown in Fig.S8, see also Fig. 2 in the main manuscript, can be well explained with the equation derived from the two-band model (Eq. (1) in the main manuscript). The values of the fit parameters should be taken, however, with some care. The mobility values we obtain between 50 K and 241 K to fit the MR field dependence shown in Fig.S8 are 3.95, 2.22 and 1.28 m^2/Vs . At lower temperatures the the-

oretical curves strongly deviate from the experimental data, which show one or two maxima in the MR at certain fields. The obtained fit values of the mobility are in agreement with published values for very thin [52] and thick [53] graphite samples. On the other hand, direct measurements of the mobility of the carriers inside the semiconducting graphene planes in thin graphite samples using micro-constrictions, provide values at least one order of magnitude larger than those obtained from the fits at similar temperatures [37]. The question whether this difference is because: (a) in thick samples the MR field dependence is mainly given by the response of the interfaces, which have a much larger carrier density ($n \sim 10^{10} \dots 10^{11} \text{ cm}^{-2}$) than in the graphene planes of the semiconducting regions ($n \lesssim 10^8 \text{ cm}^{-2}$), and/or (b) the mobility values obtained from the two-band model are incorrect because the used Eq. (1) (see main manuscript) is not, rigorously speaking, applicable when at least part of the carrier dynamic is not diffusive but ballistic [54], is not yet clarified.

V. THE HYSTERESIS IN THE MR AT HIGH MAGNETIC FIELD OBSERVED IN THICK GRAPHITE SAMPLES

The first reference for an absence of any field hysteresis in the MR between the up and down field sweeps is found in the paper of Iye et al. [9]. The authors mentioned there that because of this the magnetic field induced transitions α and α' were phase transitions of second or higher order. In the publication of Miura et al [55], high field MR measurements were done on Kish graphite. In their Fig. 1 the MR measured at 4.2 K clearly shows a field hysteresis, which begins at $\mu_0 H \approx 12$ T and ends at $\mu_0 H \approx 45$ T. However, in the manuscript this hysteresis was not mentioned and discussed. Another work published by Ochimizu et al [56] also showed a field hysteresis in the MR at different temperatures (see Fig. 2 in that publication) in a field range similar to that of Ref. 9 and ours, see Fig. 2 in our main article. Recently, Arnold et al. [41] reported the MR of bulk graphite at high magnetic fields and found sharp new features at $\mu_0 H_{\alpha'} = 52.3 \pm 0.1$ T and $\mu_0 H_{\beta'} = 54.2 \pm 0.1$ T. The authors suggested that they correspond to two distinct first order transitions associated with the abrupt depopulation of both the $(0, \uparrow)$ (electron like) and $(-1, \downarrow)$ (hole like) Landau levels. They suggested that the α' and β' are first-order transitions on the basis of the observed field hysteresis, which is shown in Fig.4(c) of that work. Independently of the theoretical explanation, our experimental results show that such hysteresis has a thickness dependence. The high fields hysteresis between up and down field sweeps is only observed at low enough temperatures and in bulk and thicker samples ($t \geq 60$ nm).

A general remark on studies under pulsed field. It is clear that heating should be always considered, i.e., whether \dot{H} might affect the result. Therefore, it is nec-

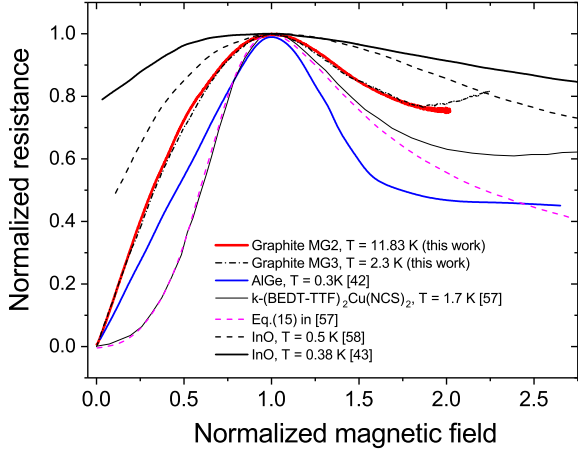


Fig.S9. Normalized resistance vs. normalized magnetic field at different constant temperatures of: graphite MG2 and MG3 samples measured in this work, with the normalization field factor at resistance maximum of $\mu_0 H^* = 27.5$ T and 30 T at 11.83 K and 2.3 K, respectively; the granular superconductor AlGe from Ref.42 with $\mu_0 H^* \simeq 2.3$ T and at 0.3 K; the organic layered superconductor κ -(BEDT-TTF)₂Cu(NCS)₂ from Ref.57 with $\mu_0 H^* \simeq 2.8$ T at 1.7 K with the voltage measured parallel to the applied field; a granular superconducting InO thin film from Ref.58 with $\mu_0 H^* \simeq 2.4$ T at 0.5 K; InO thin film from Ref. 43 with $\mu_0 H^* \simeq 3.0$ T at 0.38 K.

essary to provide the following data to assure that the hysteresis is not an artefact: (1) One needs pulsed and DC field data at the same temperature. In our case would mean to apply DC fields up to 30 T, at least, which is much above the maximum available; (2) High field and low field pulses at the same temperature; (3) Fast and slow pulses (with up/down sweeps) at the same peak field and temperature.

VI. GRANULAR SUPERCONDUCTIVITY

A key feature of the high magnetic field results in graphite samples is the maximum MR and the further negative MR observed above that maximum. As pointed out in the main manuscript and taking the normalized data of Fig.6 into account, we assume that this feature is due to the magnetic field response of certain interfaces in the graphite sample and it is not an intrinsic property of the ideal graphite stacking orders. Previous studies indicate the existence of granular superconductivity at

certain interfaces with a rather broad range of critical temperatures upon sample, see Refs. 19, 29–33, and 59. Therefore, we compare below our MR data with that obtained in granular superconductors at temperatures and fields below the critical values and in one case above the critical field.

In Fig.S9 we show the normalized MR data of the thinnest samples MG2 and MG3 at 11.83 K and 2.3 K and include the MR data of granular Al in a Ge matrix from Ref. 42, obtained at 0.3 K. It is remarkable that the normalized MR data of our MG2 and MG3 samples are practically identical, pointing to a common origin. The MR data of granular Al/Ge show a linear field dependence at low fields and a clear negative MR in a field range comparable (in normalized units) to that of the graphite samples. In the case of granular Al/Ge the field at which the negative MR regions ends is considered as the upper critical field of the superconducting grains at $\mu_0 H_{c2}(0.3K) \simeq 4.5$ T. In case of the granular InO thin films [43, 58] a similar behavior is observed although the negative MR field range has a larger extend above the maximum at $\mu_0 H^*$. The interpretation of the MR maximum, with a value larger than the resistance in the normal state at the same temperature, and the negative MR is given in terms of Josephson coupled granular superconducting grains [42]. As pointed out in Ref. 43, the negative MR at high fields can be described by a field dependent energy gap in the density of states at the Fermi level, which results from Cooper interactions. Furthermore, it has been argued that superconducting clusters at high enough fields can appear due to fluctuations [43, 45], a phenomenon that may play a role in 2D superconducting layers.

The effect of superconducting fluctuations above the critical temperature and field have been studied in detail in the last years, see Ref. 45 and Refs. therein. As example, we include in Fig. S9 the MR data of M. Kartsovnik obtained from the layered organic superconductor κ -(BEDT-TTF)₂Cu(NCS)₂ at 1.7 K with the theoretical line given in Ref. 57. One main difference with respect to the other data shown in that figure is that the MR follows a quadratic instead of a linear field dependence at low fields. Also, the theory [57] is applicable in the normal state of a granular superconductor. From all the evidence obtained during the last years in graphite we believe that the temperature where the maximum is observed are well below the critical temperature. Assuming that the field at which the negative MR ends (in AlGe that would be ~ 1.8 times the field at the maximum MR) is related to the critical field, i.e., $\mu_0 H_{c2}(0) \sim 60$ T for the granular superconducting 2D interfaces in graphite.

[1] S. Tanuma, R. Inada, A. Furukawa, O. Takahashi, and Y. Iye, “Physics in high magnetic fields,” (Springer, Berlin, 1981) p. 316.
 [2] H. Yaguchi and J. Singleton, Phys. Rev. Lett. **81**, 5193

(1998).

[3] K. Akiba, A. Miyake, H. Yaguchi, A. Matsuo, K. Kindo, and M. Tokunaga, J. Phys. Soc. Jpn. **84**, 054709 (2015).
 [4] S. Uji, J. S. Brooks, and Y. Iye, Physica B: Cond. Matt.

- 246-247**, 299 (1998).
- [5] G. Timp, P. D. Dresselhaus, T. C. Chieu, Q. Dresselhaus, and Y. Iye, *Phys. Rev. B* **28**, 7393(R) (1983).
- [6] B. Fauqué, D. LeBoeuf, B. Vignolle, M. Nardone, C. Proust, and K. Behnia, *Phys. Rev. Lett.* **110**, 266601 (2013).
- [7] T. Taen, K. Uchida, and T. Osada, *Phys. Rev. B* **97**, 115122 (2018).
- [8] T. Taen, K. Uchida, T. Osada, and W. Kang, *Phys. Rev. B* **98**, 155136 (2018).
- [9] Y. Iye, P. M. Tedrow, G. Timp, M. Shayegan, M. S. Dresselhaus, G. Dresselhaus, A. Furukawa, and S. Tanuma, *Phys. Rev. B* **25**, 5478 (1982).
- [10] Y. Iye, M. Berglund, and L. E. McNeil, *Solid State Commun.* **52**, 975 (1984).
- [11] Y. Kopelevich, B. Raquet, M. Goiran, W. Escoffier, R. R. da Silva, J. C. M. Pantoja, A. Lukyanchuk, A. Sinchenko, and P. Monceau, *Phys. Rev. Lett.* **103**, 116802 (2009).
- [12] H. Yaguchi and J. Singleton, *J. Phys.: Condens. Matter* **21**, 344207 (2009).
- [13] B. Fauqué and K. Behnia, “Basic physics of functionalized graphite,” (P. Esquinazi (ed.), Springer International Publishing AG Switzerland, 2016) Chap. 4, pp. 77–96.
- [14] D. Yoshioka and H. Fukuyama, *J. Phys. Soc. Jpn.* **50**, 725 (1981).
- [15] N. B. Brandt, G. A. Kapustin, V. G. Karavaev, A. S. Kotosonov, and E. A. Svistova, *Zh. Eksp. Teor. Fiz.* **67**, 1136 (1974).
- [16] The electrical and structural homogeneity was assumed in the literature independently whether the sample was natural graphite, highly oriented pyrolytic graphite (HOPG) or Kish graphite.
- [17] J. D. Bernal, *Proc. R. Soc. Lond. A* **106**, 749 (1924).
- [18] H. Lipson and A. R. Stokes, *Proc. R. Soc. Lond. A* **181**, 101 (1942).
- [19] P. D. Esquinazi and Y. Lysogorskiy, “Basic physics of functionalized graphite,” (P. Esquinazi (ed.), Springer International Publishing AG Switzerland, 2016) Chap. 7, pp. 145–179.
- [20] I. Brihuega, P. Mallet, H. González-Herrero, G. T. de Laissardière, M. M. Ugeda, L. Magaud, J. M. Gómez-Rodríguez, F. Ynduráin, and J.-Y. Veullen, *Phys. Rev. Lett.* **109**, 196802 (2012).
- [21] W. A. Muñoz, L. Covaci, and F. M. Peeters, *Phys. Rev. B* **87**, 134509 (2013).
- [22] N. B. Kopnin and T. T. Heikkilä, “Carbon-based superconductors: Towards High- T_c superconductivity,” (Pan Stanford Publishing, CRC Press, Taylor & Francis Group, 2015) Chap. 9, pp. 231–263, arXiv:1210.7075.
- [23] J. C. Gonzalez, M. Muñoz, N. García, J. Barzola-Quiquia, D. Spoddig, K. Schindler, and P. Esquinazi, *Phys. Rev. Lett.* **99**, 216601 (2007).
- [24] Y. Ohashi, T. Hironaka, T. Kubo, and K. Shiiki, *TANSO* **195**, 410 (2000).
- [25] Y. Ohashi, K. Yamamoto, and T. Kubo, Carbon’01, An International Conference on Carbon, Lexington, KY, United States, July 14-19, Publisher: The American Carbon Society, available at www.acs.omnibooksonline.com, 568 (2001).
- [26] Y. Zhang, J. P. Small, M. E. S. Amori, and P. Kim, *Phys. Rev. Lett.* **94**, 176803 (2005).
- [27] J. Barzola-Quiquia, J.-L. Yao, P. Rödiger, K. Schindler, and P. Esquinazi, *Phys. Stat. Sol. (a)* **205**, 2924 (2008).
- [28] M. Zoraghi, J. Barzola-Quiquia, M. Stiller, P. D. Esquinazi, and I. Estrela-Lopis, *Carbon* **139**, 1074 (2018).
- [29] Y. Cao, V. Fatemi, S. Fang, K. Watanabe, T. Taniguchi, E. Kaxiras, and P. Jarillo-Herrero, *Nature* **556**, 43 (2018).
- [30] A. Ballestar, J. Barzola-Quiquia, T. Scheike, and P. Esquinazi, *New J. Phys.* **15**, 023024 (2013).
- [31] A. Ballestar, T. T. Heikkilä, and P. Esquinazi, *Superc. Sci. Technol.* **27**, 115014 (2014).
- [32] A. Ballestar, P. Esquinazi, and W. Böhlmann, *Phys. Rev. B* **91**, 014502 (2015).
- [33] C. E. Precker, P. D. Esquinazi, A. Champi, J. Barzola-Quiquia, M. Zoraghi, S. Muiños-Landin, A. Setzer, W. Böhlmann, D. Spemann, J. Meijer, T. Muenster, O. Baehre, G. Kloess, and H. Beth, *New J. Phys.* **18**, 113041 (2016).
- [34] N. García, P. Esquinazi, J. Barzola-Quiquia, and S. Dusari, *New Journal of Physics* **14**, 053015 (2012).
- [35] M. Zoraghi, J. Barzola-Quiquia, M. Stiller, A. Setzer, P. Esquinazi, G. H. Kloess, T. Muenster, T. Lühmann, and I. Estrela-Lopis, *Phys. Rev. B* **95**, 045308 (2017).
- [36] J. C. González, M. Muñoz, N. García, J. Barzola-Quiquia, D. Spoddig, K. Schindler, and P. Esquinazi, *Phys. Rev. Lett.* **99**, 216601 (2007).
- [37] S. Dusari, J. Barzola-Quiquia, P. Esquinazi, and N. García, *Phys. Rev. B* **83**, 125402 (2011).
- [38] P. Esquinazi, J. Barzola-Quiquia, S. Dusari, and N. García, *J. Appl. Phys.* **111**, 033709 (2012).
- [39] B. T. Kelly, *Physics of Graphite* (London: Applied Science Publishers, 1981).
- [40] Y. Kopelevich, J. H. S. Torres, R. R. da Silva, F. Mrowka, H. Kempa, and P. Esquinazi, *Phys. Rev. Lett.* **90**, 156402 (2003).
- [41] F. Arnold, A. Isidori, E. Kampert, B. Yager, M. Eschrig, and J. Saunders, *Phys. Rev. Lett.* **119**, 136601 (2017).
- [42] A. Gerber, A. Milner, G. Deutscher, M. Karpovsky, and A. Gladkikh, *Phys. Rev. Lett.* **78**, 4277 (1997).
- [43] V. F. Gantmakher, M. V. Golubkov, V. T. Dolgopolo, J. G. S. Lok, and A. K. Geim, *JETP* **82**, 951 (1996).
- [44] I. S. Beloborodov, A. V. Lopatin, V. M. Vinokur, and K. B. Efetov, *Reviews of Modern Physics* **79**, 469 (2007).
- [45] A. A. Varlamov, A. Galda, and A. Glatz, *Rev. Mod. Phys.* **90**, 015009 (2018).
- [46] P. Esquinazi, N. García, J. Barzola-Quiquia, P. Rödiger, K. Schindler, J.-L. Yao, and M. Ziese, *Phys. Rev. B* **78**, 134516 (2008).
- [47] A. Ballestar, P. Esquinazi, J. Barzola-Quiquia, S. Dusari, F. Bern, R. da Silva, and Y. Kopelevich, *Carbon* **72**, 312 (2014).
- [48] A. Simons, A. Gerber, I. Y. Korenblit, A. Suslov, B. Raquet, M. Passacantando, L. Ottaviano, G. Impellizzeri, and B. Aronzon, *Journal of Applied Physics* **115**, 093703 (2014).
- [49] T. Khouri, U. Zeitler, C. Reichl, W. Wegscheider, N. E. Hussey, S. Wiedmann, and J. C. Maan, *Phys. Rev. Lett.* **117**, 256601 (2016).
- [50] Y. Kopelevich, J. H. S. Torres, R. R. da Silva, F. Mrowka, H. Kempa, and P. Esquinazi, *Phys. Rev. Lett.* **90**, 156402 (2003).
- [51] Y. Kopelevich, P. Esquinazi, J. H. S. Torres, R. R. da Silva, and H. Kempa, “Graphite as a highly correlated electron liquid,” (B. Kramer (Ed.), Springer-Verlag Berlin, 2003) pp. 207–222.

- [52] Y. Zhang, J. P. Small, M. E. S. Amori, and P. Kim, *Phys. Rev. Lett.* **94**, 176803 (2005).
- [53] K. Noto and T. Tsuzuku, *Japanese Journal of Applied Physics* **14**, 46 (1975).
- [54] N. García, P. Esquinazi, J. Barzola-Quiquia, B. Ming, and D. Spoddig, *Phys. Rev. B* **78**, 035413 (2008).
- [55] N. Miura, H. Ochimizu, T. Takamasu, S. Takeyama, and S. Sasaki, *Physica B* **177**, 505 (1992).
- [56] H. Ochimizu, T. Takamasu, S. Takeyama, S. Sasaki, and N. Miura, *Phys. Rev. B* **46**, 1986 (1992).
- [57] A. Glatz, A. A. Varlamov, and V. M. Vinokur, *Phys. Rev. B* **84**, 104510 (2011).
- [58] Y. Lee, A. Frydman, T. Chen, B. Skinner, and A. M. Goldman, *Phys. Rev. B* **88**, 024509 (2013).
- [59] M. Stiller, P. D. Esquinazi, J. Barzola-Quiquia, and C. E. Precker, *J. Low Temp. Phys.* **191**, 105 (2018).